Innovative Experimental Low Cost Electronics Operated Instrumentation for Wearable Health Systems with High Resolution Physiological Measurements

D.F. Cruz, E.M.G. Rodrigues, R. Godina, C.M.P. Cabrita
UBI and CISE, Covilha, Portugal
daniel.fonseca.cruz@gmail.com; erodrigues0203@gmail.com; radugodina@gmail.com; cabrita@ubi.pt

J.C.O. Matias
DEGEIT, Univ. Aveiro, and C-MAST/UBI, Covilha, Portugal
jmatias@ua.pt

J.P.S. Catalão
INESC TEC and FEUP, Porto, C-MAST/UBI, Covilha, and INESC-ID/IST, Lisbon, Portugal
catalao@fe.up.pt

***Abstract*—The aim of this paper is to present the development of an innovative experimental reflective pulse oximetry solution targeting wearable health system for daily monitoring purposes. The measurement of two common human physiological indicators is performed, which are the pulse rate and the blood oxygenation level (SpO_2). The design options are detailed, covering photoplethysmographic (PPG) signals sensing architecture and post-processing digital filter operations. The high resolution of the physiological measures is achieved using sigma delta conversion technique. Conclusions are duly drawn.**

Keywords—Wearable health systems; Reflective pulse oximeter; Biomedical sensor; Signal acquisition; Digital signal processing;

I. INTRODUCTION

One non-invasive medical tool that is capable to measure the SpO_2 and the pulse rate level in the blood of a patient is the pulse oximeter. Patients with pulmonary or cardiac diseases may measure their blood oxygenation uninterruptedly, for instance while doing physical exercise or jogging [1]. Distinctive miniaturised profitable pulse oximeter systems are currently available, which can be transported around by the patient under investigation. However, measurements are typically made at the extremities of the body. Consequently, the sensor is applied to peripheral parts of the human body [2].

Nowadays, several diverse versions of pulse oximeters in the market are available. They vary in quality, size, and cost. The oximeters with a certain complexity utilised in hospitals are normally non portable and outsized. Nevertheless, many handheld pulse oximeters currently exist for domestic applications such as remarkably compact and simple to operate. The most common type is the model of the finger, that exhibits the SpO_2 and pulse rate [3].

The wrist-finger model is noticeably ordinary in the market as well. The appliance is in fact a finger model since the sensor is positioned on a finger which is consequently attached to a wrist display. However, the pulse oximeter on the finger is relatively visible and the finger might not be entirely comfortable for extended periods and nonstop monitoring [1]. Still, there are some disadvantages such as the recurrent addition of movement artefacts intercede particularly with long term monitoring of a subject.

Another shortcoming is the low quality of the signal in the incident of centralization in cases in which the subject suffers from sepsis, coldness, shock or cardio-pulmonary anomalies. On the other hand, such occurrences are the highest application scenarios of portable SpO_2 monitors [4].

There are two types of pulse oximeters available: of the reflection nature and the transmission nature. When the two categories are compared, the reflection one appears to be more capable since is possible to measure any area on the skin surface. Conversely, in the case of oximeters of reflection nature, the reasonably great background (BG) light incident on the light detector and the poor reflection signal acquired from the skin surface exclude precise measurements [5].

The objective of this research work is to present the development of an experimental pulse reflective based wearable health system for daily monitoring covering. In this sense, we report and demonstrate its application through the means of two indicators which are the pulse rate and the SpO_2. The design options are detailed covering not only the analog front end (AFE) architecture as well as post-processing digital filter operations. The high resolution of the physiological measures is achieved using sigma delta conversion technique.

The paper is organised as follows. The pulse oximetry theory is described in Section II. Section III describes briefly portable oximetry device requirements for wearable applications. Section IV details system design. Section V contains the tests performed on the prototype board and provides results discussion. Finally, the conclusions are summarized in Section V.

II. PULSE OXIMETRY PRINCIPLES

When the oxygen (O_2) is in the blood it can be transported in two ways. It can be dissolved in the plasma, which corresponds to 2% of the total value, the reason being that the blood is made essentially by water and that the gases hardly dissolve in such environments. A second and more efficient way is the connection of O_2 to the hemoglobin [6]. The saturation of HbO_2 or the functional saturation of O_2 is calculated as follows:

$$SO_2(\%) = \frac{[HbO_2]}{[HbO_2]+[Hb]} \times 100\% \quad (1)$$

978-1-5090-2320-2/16/$31.00 ©2016 IEEE

Generally, reflectance pulse oximetry operates with two different wavelengths through a tissue with the purpose of measuring the transmitted light signal. Thus, its operation is based on physical principles concerning behaviour of the light. The values in which the absorption of HbO_2 and Hb present the highest difference of absorption are chosen [7]. Another method is the flattening of the absorption spectrum that aims to minimize the errors associated with the modification of wavelength peaks of the sensor LEDs [8]. The red (RED) band (660nm) and infrared (IR) (880-940nm) are the wavelengths usually used for pulse oximetry. Such wavelengths are selected due to the reason of maximizing absorption and limit the margin of error of the device [9]. LEDs can emit wavelength of different intensities, thus, a standardization of such intensities has to be made. Since the signal DC bias is common for different wavelengths it is possible to obtain a ratio (R) between the emitted light of the red and infrared LED [10]. The HbO2 saturation is estimated by:

$$R = \frac{log_{10}\left(\frac{I_{DC+AC}}{I_{DC}}\right)_V}{log_{10}\left(\frac{I_{DC+AC}}{I_{DC}}\right)_{IV}} = \frac{log_{10}\left(I_{AC}\right)_V}{log_{10}\left(I_{AC}\right)_{IV}} \quad (2)$$

and by combining equation (2) with the following equations known as the Lambert-Beer law:

$$I_t = I_0 \times e^{-A} \quad (3)$$

$$A = \varepsilon \times D \times c \quad (4)$$

the equation (5) of SO_2 is obtained:

$$SO_2 = \left\{-\varepsilon_V(Hb) + \varepsilon_{IV}(Hb) \times \left(\frac{V}{IV}\right)\right\} \times \left\{\left[\varepsilon_V(HbO_2) - \varepsilon_V(Hb)\right] + \left[\varepsilon_{IV}(Hb) - \varepsilon_{IV}(HbO_2)\right] \times \left(\frac{V}{IV}\right)\right\}^{-1} \quad (5)$$

where I_t is the intensity of light that trespasses the medium, I_0 represents the intensity of incident light, A is the absorbance, D represents the distance covered beam of light, ε is the extinction coefficient and c represents the concentration of the solution. Even though the Lambert-Beer law is a great basis for pulse oximetry, there are some unforeseen occasions when the measurement of SO_2 doesn't follow the law [9].

Since part of the transmitted light is reflected by the blood cells different methods of calibration of oximeters were created, the most used one being tables with reference values based on studies with volunteers, where the SO_2 is measured by a medical device through an invasive manner [11]. Many studies were made with the aim to minimize the errors associated to such type of measurement resulting in a modification of the SO_2 equation. The relation between R and the measured values by the oximeter are made by [7]:

$$SpO_2 = \frac{K_1 - K_2 R}{K_3 - K_4 R} \quad (6)$$

The K coefficients are obtained experimentally, through in vitro measurements for the best approximation possible [9].

III. Compact Design Solution for Wearable Oximetry Instrumentation

Conventional portable oximetry systems are typically built using excitation led units, a photodetector interface circuit and a precision analog digital converter (ADC) module operated by a microcontroller (MCU) that extract the AC and DC components of the plethysmography signals. Despite the small size of the components discrete circuitry a considerable print circuit board area is required. In order to address today trends toward smaller electronics devices without compromising the performance, efforts have been made to integrate as much as possible the various elements of the dedicated circuitry in miniature form into a single silicon unit. This kind of high integration and specialized circuitry is known as System on Chip (SoC).

For wearable health applications the oximetry technology should present very small form factor without causing discomfort with its use. Furthermore, to be portable its weight should be minimized and its energy consumption profile very restricted which can be considered challenging due to the LED sources [7].

Reflected PPG signals measurement devices as an alternative to transmission pulse oximetry may achieve these qualifications while offering a singular advantage that enable them to be located in different body areas [12]. Several semiconductor manufacturers are targeting this market releasing sophisticated SoC units for this purpose. The high miniaturization level means that a very capable wearable monitoring system comprising a MCU, biomedical sensors and advanced wireless communication features can be merged into a very small physical device.

The level of miniaturization is illustrated in Fig. 1 where is compared the transmission pulse oximetry designed conventional solution versus the SoC unit that incorporates a reflective PPGs measurement biomedical sensor.

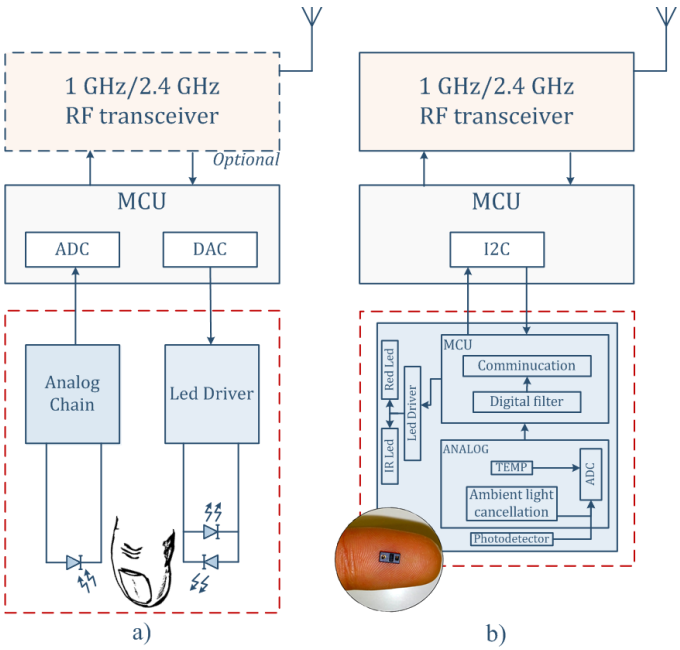

Fig. 1. Two design approaches: a) discrete components based conventional design b) High integration solution based on dedicated oximeter SoC.

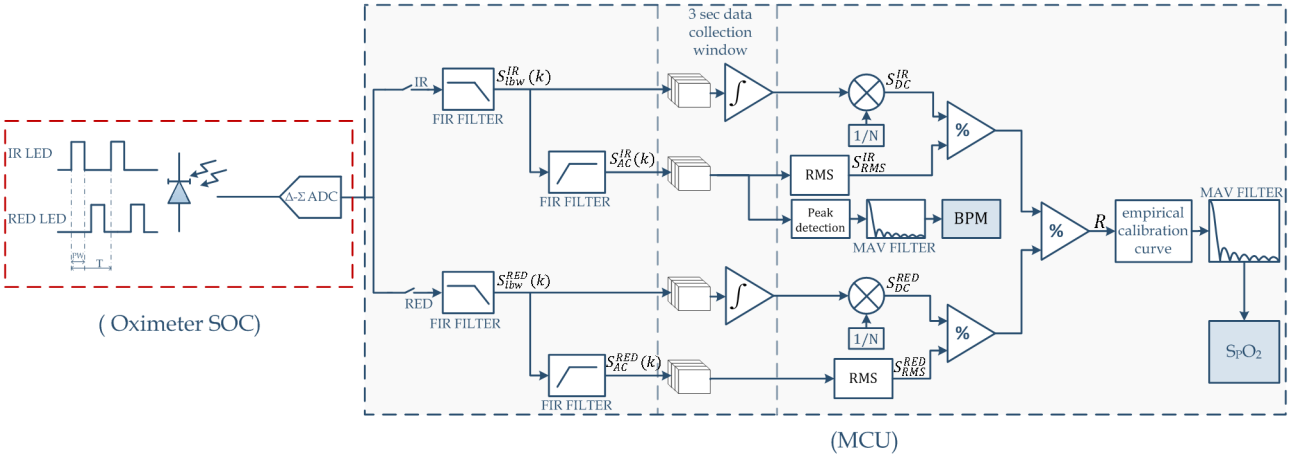

Fig. 2. Global view of core algorithms performed inside MCU.

One important feature of the integrated pulse oximetry is evident by requiring less internal MCU resources since PPGs acquisition and basic signal processing is handled by the SoC. In this sense, the MCU peripheral system can be downsized saving silicon area, thus contributing to a high compact biomedical sensor solution.

IV. System Architecture

A. The SoC device

The reflectance pulse oximeter design in discussion relies on a MAX30100 SoC unit manufactured by Maxim Integrated [13]. It offers two LEDs, photodetector, low-noise analog signal processing functions to minimize ambient light impact and a 16-bit sigma delta ADC. PPGs sampling rate varies between 50sps and 1000sps. Conversion dynamic range depends on LED current pulse width. Highest pulse width enables 16-bit digital conversion. Setting the minimum pulse width conversion output does not surpass 13-bit of resolution.

B. MCU core based Signal processing algorithms

Significant signal extraction and noise reduction techniques are already taken by the oximeter SoC. However, there is scope for improving the quality of readings if the goal is to maximize high-fidelity PPGs with the existing hardware resources. The block diagram in Fig. 2 highlights the post-processing operations performed by the MCU. The signal processing main tasks consist of white noise filtering, DC component measurement and AC term extraction of the PPGs.

In Fig. 2 the upper digital signal processing chain refers to the signal treatment carried out with IR signals acquired through the SoC's ADC module. The same set of operations is implemented in the lower signal chain, with the exception of the heart rate measurement (BPM) block which is performed solely on the IR PPGs AC components.

The maximum dynamic range provided by the oximeter SoC is 16-bit configured for 50sps the lowest sampling rate available. The low acquisition rate simplifies any intensive math-intensive applications to be run within a MCU.

To analyze the post-processing requirements important information can be extracted if the discrete Fourier transform (DFT) algorithm is applied to the PPG raw data sent.

The equation for an N-point DFT has the form:

$$X(m) = \sum_{n=0}^{N-1} x(n) e^{-j2\pi mn/N} \quad M = 0,\ldots N-1 \qquad (7)$$

where $x(n)$ is the sequence of raw PPG samples, N is the number of samples used for computing the DFT output, n is the index of the time-domain index of the incoming samples and m the DTF output index in the frequency domain. A time-series of approximately 26s was collected and analyzed via DFT. The DFT bin resolution is provided by 1310 samples. By taking the magnitude squared of each $X(m)$ term, the power spectrum of both PPG values is shown in Fig. 3.

According to the figure the spectral content is present close to 10 Hz. As expected, the arterial pulsating part is considerable low in comparison to absorption component due to remaining tissue. For SpO_2 evaluation usable bandwidth starts at 0Hz and superiorly limited by the maximum heart rate measurement requirement. Normally, professional heart rate monitoring devices are designed to read up to 300 bpm. Thus practical bandwidth of interest goes as maximum as 5 Hz. Thus, additional frequency removal efforts can be made applying low pass digital filtering by removing unnecessary frequency. For the design in discussion the low pass filter cut-off frequency is set at 3 Hz and stopband starts at 6 Hz. That implies heart rate tracking is functional up to 180 bpm. Filter stop band level is set at -105 dB. The results can be observed in Fig. 4. Above 3 Hz the remaining harmonic signature is rapidly attenuated in amplitude being a result of the roll-off imposed by the low-pass digital filtering specifications. Furthermore, white noise resulted from quantization process is minimized.

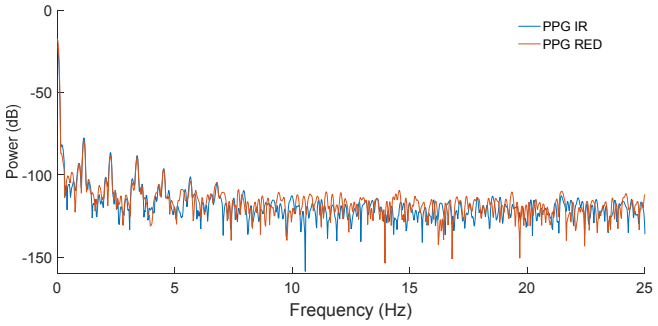

Fig. 3. Power spectrum of acquired PPG signals sampled at f_s= 50 sps.

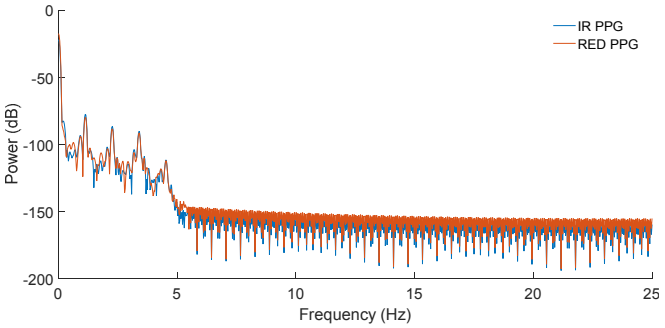

Fig. 4. PPG signals power spectrum after applying a low pass digital filter.

It should be noticed that the effective ADC conversion noise floor is not given by the DFT noise floor. Therefore, DFT processing has to be subtracted from the power spectrum figures [14]. For heart rate measurement only the periodicity of the AC term is of interest, a high pass digital filter guarantees that the slow exponential decay of the PPG signals is completely removed. The discrete structure is configured with the stopband corner frequency set at 0.20 Hz while the lower passband frequency is 0.80Hz. The DC tracker blocks in Fig. 2 determine the photocurrent DC level for each PPG signal. For that, data are collected and passed through a first-order IIR digital integrator. A trapezoidal rule time-domain integration approximation is chosen due to the property of showing linear phase similar to an ideal digital frequency response [14]. The transfer function is defined by:

$$H_{Tr}(z) = \frac{T_s}{2}\left(\frac{1+z^{-1}}{1-z^{-1}}\right) \tag{8}$$

where T_s is the sampling period.

Finally, a moving average filter (MAF) is the last signal processing function to be applied. Both the quantities, that is, the BPM and SpO_2 outputs are smoothed in order to limit any glitch that could jeopardize the results over the last computed estimations. For such purpose, each most recent result is averaged with the last 5 SpO_2 calculations. Since the number of samples used for this operations is fixed by a window length T_w, its frequency-dependent attenuation characteristic has no impact if the MAF averages a short series of time-domain results. Therefore, the MAF keeps a fast transient response. The Z-domain based discrete representation as follows [15]:

$$H_{MAF}(z) = \frac{1}{N}\left(\frac{1-z^{-N}}{1-z^{-1}}\right) \tag{9}$$

and where N is:

$$N = \frac{T_w}{T_s} \tag{10}$$

V. Experimental Evaluation

A. Prototype design

The oximeter prototype comprises a 32-bit MCU, the MAX30100 SoC and two external power management units that supply 1.8V and 3.3 voltage rails.

The digital signal processing tasks for limiting wideband noise and to confine the sampled PPG signals to the useful bandwidth of the input signals are performed by a TM4C123 series microcontroller from Texas Instruments. Fig. 5 depicts the main components of the prototype board.

For the sake of clarity, raw and post-processed photo-detector readings along with the SpO_2 and BPM estimations are sent to an application developed in Matlab environment. The Matlab operated graphical user interface (MGUI) allows an easy configuration since the MAX30100 SoC has varying number of parameters for its internal operation. The data received by MGUI is acquired in real time through the MCU I2C interface that acts as a virtual com port. Oscilograms of the raw PPGs or post-filtered can be visualized during the tests, enabling the crossing of data being acquired. A general view of the MGUI can be seen in Fig. 6.

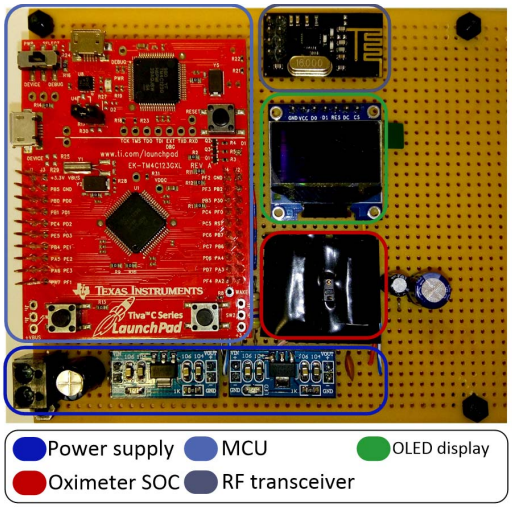

Fig. 5. Reflectance pulse oximeter test board.

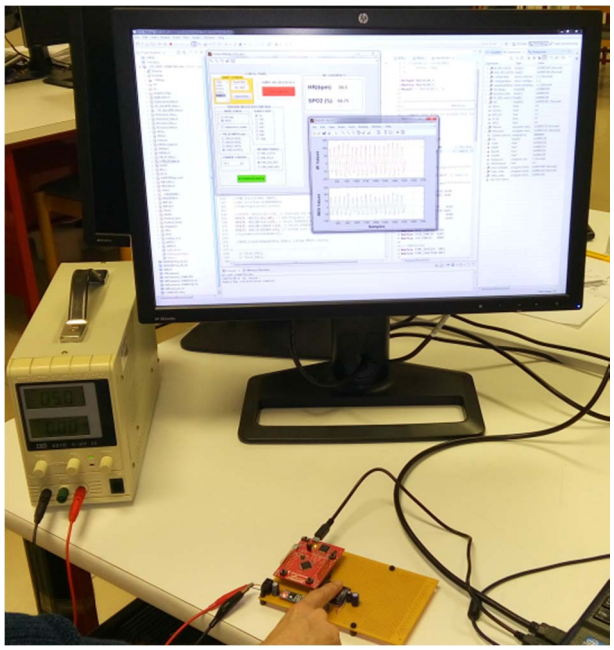

Fig. 6. Prototype board in operation sending real time data to MGUI application.

B. Results and discussion

The signal quality of readings is evaluated exploring a set of LED driving currents. Photoplethysmogram tests were carried out covering 20 seconds of acquisitions on a single male subject. At this phase of development, the experimental characterization is confined to fingertip based measurements by the reason of being a body area where the arterial supply is significant. Data collected for prototype characterization consists of raw PPG signals and AC component extraction plots. LED Pulse width control is fixed and set for 1600us and cyclical activity alternate with a period of 20ms.

It is clear from Figs 7-9 that the DC and AC components signal level is affected by the LED current peak intensity. The slow exponential decay of the PPG signals has a higher average value when driving LED light sources near its maximum current (50mA). Lowering the driving current, the photocurrent detected becomes more noise. From a signal-to noise (SNR) view point readings are resolved with lesser granularity due to electronic noise in the SoC's AFE by using low driving currents. On the other hand, it should be noticed that a higher led current may relief the low-pass digital filtering requirements for attenuating ADC quantization noise negative contribution and photodetector circuit noise performance. Thus, choosing the right LED current value is a matter of trade-off if the energy consumption is a vital concern.

An overview of Figs. 10-12 reveals the same trend for the AC term. The peak-to-peak amplitude grows as the LED current rises from 7.6mA to 40.2mA. Considering the use of ADC full range, at the highest LED current configuration AC component is resolved with approximately 7.7 bits. By minimizing the LED current under examination (7.6mA) it is not possible to get more than 5.5 bits. In this analysis it was considered the worst AC readings scenario where the AC RED reading is lower comparatively to AC IR PPG reading. Computing the ratio between the pulsatile AC component and DC term based on the sampled photocurrent readings (R_{IR} and R_{RED}), the IR PPGs generated ratio value is approximately the double of the ratio calculated with the RED PPG signals. In the latter case AC term is 0.68%-0.72% of the DC component while the IR readings AC component is 0.96%-1.5% of the respective DC component.

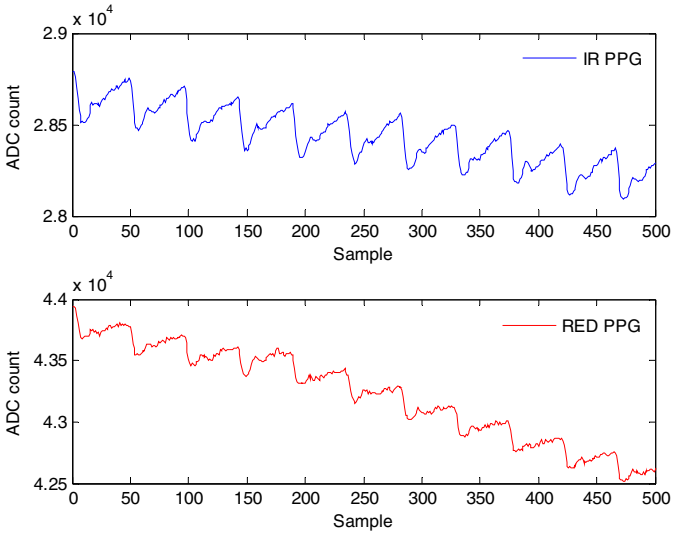

Fig. 7. Raw acquisitions with a 40.2mA peak pulsed LED current.

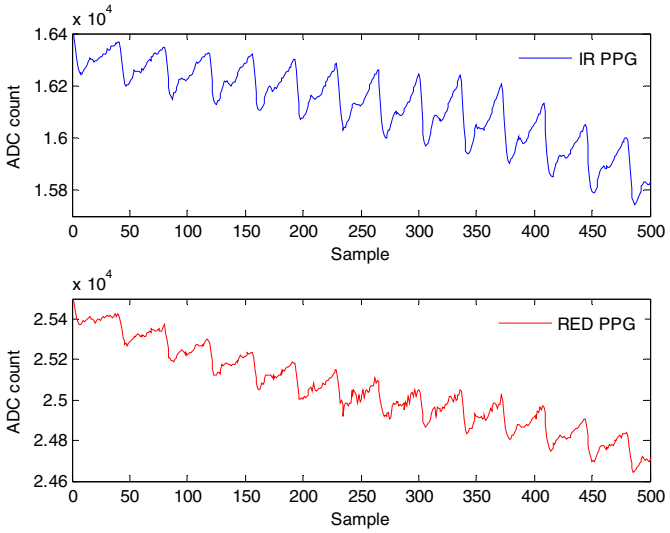

Fig. 8. Raw acquisitions with a 20.8mA peak pulsed LED current.

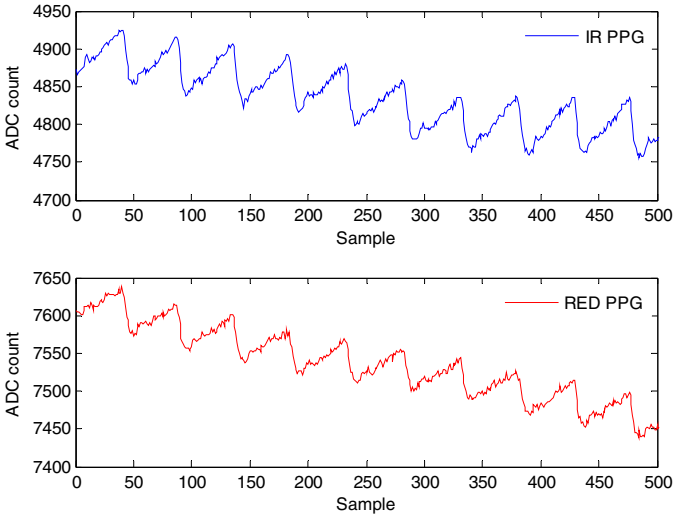

Fig. 9. Raw acquisitions with a 7.6mA peak pulsed LED current.

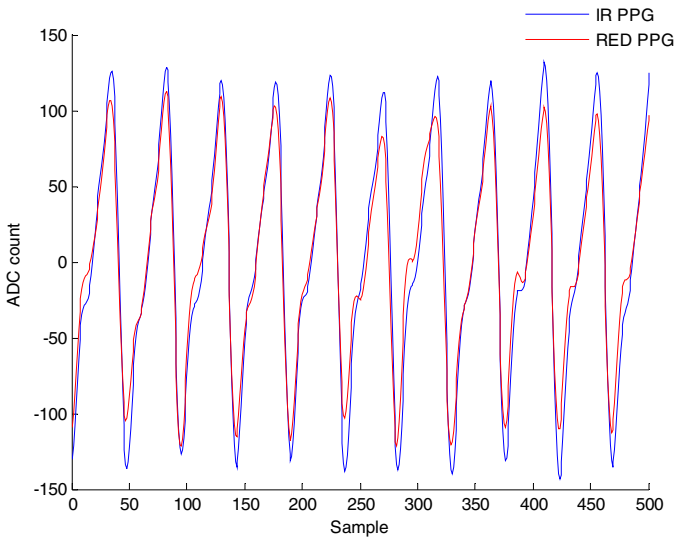

Fig. 10. Photocurrent AC component generated with 40.2mA peak pulsed LED current.

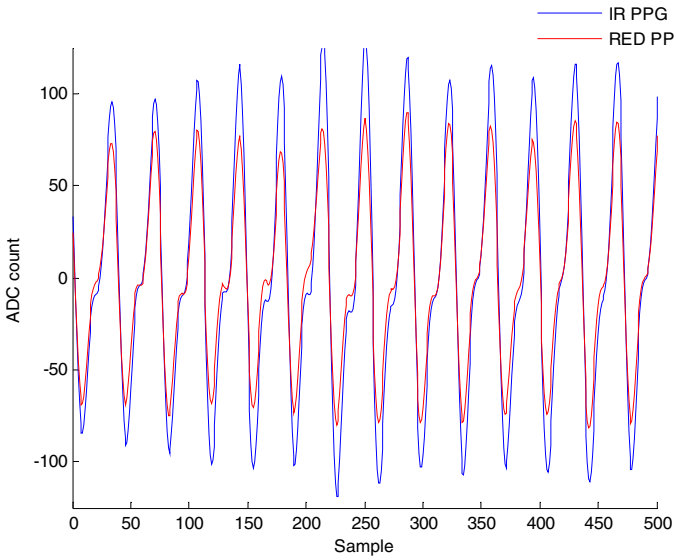

Fig. 11. Photocurrent AC component generated with 20.8mA peak pulsed LED current.

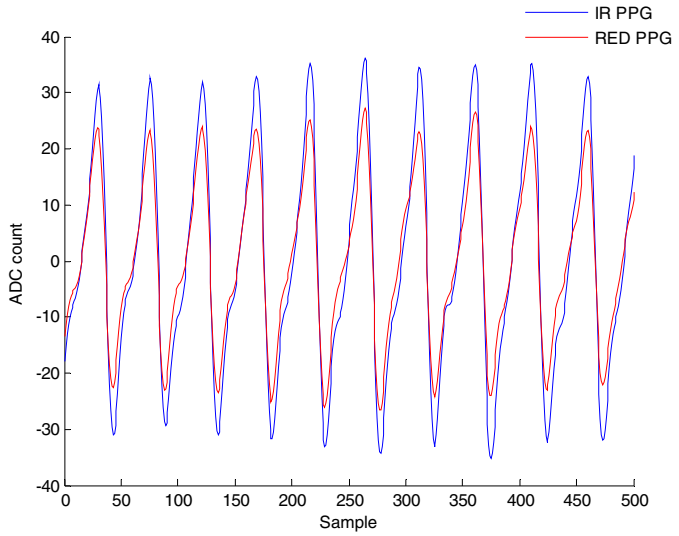

Fig. 12. Photocurrent AC component generated with 7.6mA peak pulsed LED current.

VI. Conclusion

The basis for a high compact pulse oximetry sensor has been presented having as core a dedicated oximeter SoC. The oximeter under evaluation senses the PPG signals by reflective pulse oximetry as an alternative to transmission pulse oximetry design. A prototype board was developed and tested in laboratory. The set of tests were performed collecting measurements with the highest dynamic range provided by the SoC device. The DC and pulsatile AC components sensitivity of the PPG signals to different LED current values were investigated.

Acknowledgment

This work was supported by FEDER funds through COMPETE and by Portuguese funds through FCT, under FCOMP-01-0124-FEDER-020282 (Ref. PTDC/EEA-EEL/118519/2010) and UID/CEC/50021/2013, and also by funds from the EU 7th Framework Programme FP7/2007-2013 under GA no. 309048.

References

[1] G. Pang and C. Ma, "A Neo-Reflective Wrist Pulse Oximeter," IEEE Access, vol. 2, pp. 1562-1567, 2014.

[2] M. Khan, C. G. Pretty, A. C. Amies, R. Elliott, Y. S. Chiew, G. M. Shaw and J. G. Chase, "Analysing the effects of cold, normal, and warm digits on transmittance pulse oximetry," Biomedical Signal Processing and Control, vol. 26, pp. 34-41, 2016.

[3] A. Dixit, R. Sharma and S. Barai, "Developing and Prototyping Pulse Oximeter for Elderly People," Materials Today: Proceedings, vol. 2, no. 4–5, pp. 1560-1567, 2015.

[4] M. Hülsbusch, V. Blazek, M. Herzog, S. Vogel, T. Wartzek, D. Starke and T. Hennig, "Development of a miniaturized in-ear pulse oximeter for long term monitoring of risk patients," in IFMBE Proceedings World Congress on Medical Physics and Biomedical Engineering, Munich, Germany, 2009.

[5] T. Miyata, T. Iwata and T. Araki, "A Reflection-Type Pulse Oximeter Using Four Wavelengths Equipped with a Gain-Enhanced Gated-Avalanche-Photodiode," in 13th International Conference on Biomedical Engineering - ICBME, Singapore, 2008.

[6] O. Guven, F. Geier, D. Banks and C. Toumazou, "An open-source platform for the development of microcontroller based multi-wavelength oximetry," in 2010 Biomedical Circuits and Systems Conference (BioCAS), Paphos, 2010.

[7] S. V. Gubbi and B. Amrutur, "Adaptive Pulse Width Control and Sampling for Low Power Pulse Oximetry," IEEE Transactions on Biomedical Circuits and Systems, vol. 9, no. 2, pp. 272-283, 2015.

[8] B. Venema, J. Schiefer, V. Blazek, N. Blanik and S. Leonhardt, "Evaluating Innovative In-Ear Pulse Oximetry for Unobtrusive Cardiovascular and Pulmonary Monitoring During Sleep," IEEE Journal of Translational Engineering in Health and Medicine, vol. 1, pp. 2700208-2700208, 2013.

[9] L. S. Lovinsky, "Urgent problems of metrological assurance of optical pulse oximetry," IEEE Transactions on Instrumentation and Measurement, vol. 55, no. 3, pp. 869-875, 2006.

[10] E. A. Pelaez and E. R. Villegas, "LED power reduction trade-offs for ambulatory pulse oximetry," in 2007 29th Annual International Conference of the IEEE Engineering in Medicine and Biology Society, Lyon, 2007.

[11] Y. Pole, "Evolution of the pulse oximeter," International Congress Series, vol. 1242, pp. 137-144, 2002.

[12] J. A. Sukor, M. S. Mohktar, S. J. Redmond and N. H. Lovell, "Signal Quality Measures on Pulse Oximetry and Blood Pressure Signals Acquired from Self-Measurement in a Home Environment," IEEE Journal of Biomedical and Health Informatics, vol. 19, no. 1, pp. 102-108, 2015.

[13] Maxim Integrated Products, Inc, "MAX30100 - Pulse Oximeter and Heart-Rate Sensor IC for Wearable Health," 2014.

[14] R. G. Lyons, Understanding Digital Signal Processing, Michigan: Prentice Hall, 2010.

[15] S. Golestan, M. Ramezani, J. M. Guerrero, F. D. Freijedo and M. Monfared, "Moving Average Filter Based Phase-Locked Loops: Performance Analysis and Design Guidelines," IEEE Transactions on Power Electronics, vol. 29, no. 6, pp. 2750-2763, 2014.